

# First Infrared Spectroscopic Detection of the Monobridged Diboranyl Radical ( $B_2H_5$ , $C_{2v}$ ) and Its D5-Isotopomer in Low-Temperature Diborane Ices

Jonilyn G. Longenecker,<sup>†</sup> Alexander M. Mebel,<sup>‡</sup> and Ralf I. Kaiser<sup>\*†</sup>

Department of Chemistry, University of Hawai'i at Manoa, Honolulu, Hawaii 96822, and Department of Chemistry and Biochemistry, Florida International University, Miami, Florida 33199

Received November 29, 2006

With the use of a surface-scattering machine, layers of  $27 \pm 4$  nm diborane ( $B_2H_6$ ) frosts were irradiated at 10 K and  $10^{-10}$  Torr with energetic electrons. The electrons induce a unimolecular decomposition of the diborane molecules and lead to boron–hydrogen bond rupture processes. Here, we report the first infrared spectroscopic detection of the monobridged diboranyl radical ( $B_2H_5$ ,  $C_{2v}$ ) via the  $\nu_8$  mode at  $1033\text{ cm}^{-1}$ . The infrared assignment of the  $B_2H_5$  isomer was verified by conducting experiments with diborane- $d_6$  ( $B_2D_6$ ). Under identical experimental conditions, the monobridged  $B_2D_5$  isomer was observed via the  $\nu_6$  ( $1154\text{ cm}^{-1}$ ),  $\nu_8$  ( $823\text{ cm}^{-1}$ ), and  $\nu_5$  ( $1307\text{ cm}^{-1}$ ) absorptions. These data can be utilized in future spectroscopic studies of chemical vapor deposition processes to allow an identification of the monobridged diboranyl isomer in real time via infrared spectroscopy.

## 1. Introduction

In recent years, diborane ( $B_2H_6$ ) has become the most industrially common boron-containing precursor within the growing field of chemical vapor deposition (CVD). Because of the applicability of diborane as a noncorrosive semiconductor and its resistance to degradation at high temperatures, it can be effectively used in the production of intrinsic devices and electrochemical sensors.<sup>1</sup> In this context, understanding the molecular energetics and spectroscopic properties of the reacting, boron-containing materials is crucial in CVD processes to obtain accurate rate constants, determine thermodynamic data, and predict products. Thus, in order to understand fundamental diborane reactions in boron-doped CVD processes, the spectroscopic identification of boron-bearing reaction intermediates such as the diboranyl radical ( $B_2H_5$ ) is essential.

Diborane also has theoretically intriguing characteristics in addition to commercial uses. After identification of the dibridged three-center, two-electron structure of the diborane

molecule, multiple studies were undertaken to determine structural and energetic characteristics of this unique compound. One crucial query was whether hydrogen is abstracted more readily from the terminal position of diborane in a reaction yielding dibridged  $B_2H_5$  or from the bridging position forming the monobridged  $B_2H_5$  isomer (Figure 1). The terminal position is more accessible for abstraction and holds a larger cone of acceptance; however, the chemical bonding at the bridging position is less stable. Early experimental results obtained by Manocha et al. and Ruščić et al. indicated that  $B_2H_5$  is most stable as the singly bridged structure.<sup>2,3</sup> Since that time, multiple theoretical studies have confirmed these results; the  $C_{2v}$  symmetric monobridged  $B_2H_5$  isomer now is universally accepted as the lowest-energy isomer being about  $20\text{ kJ mol}^{-1}$  more stable than the dibridged,  $C_s$  symmetric  $B_2H_5$  radical.<sup>4–7</sup>

\* To whom correspondence should be addressed. E-mail: kaiser@gold.chem.hawaii.edu.

<sup>†</sup> University of Hawai'i at Manoa.

<sup>‡</sup> Florida International University.

(1) Comerford, D. W.; Cheesman, A.; Carpenter, T. P. F.; Davies, D. M. E.; Fox, N. A.; Sage, R. S.; Smith, J. A.; Ashfold, M. N. R.; Mankelevich, Y. A. *J. Phys. Chem. A* **2006**, *110*, 2868 and references therein.

(2) Manocha, A. S.; Setser, D. W.; Wickramaartchi, M. A. *J. Chem. Phys.* **1983**, *76*, 129.

(3) Ruščić, B.; Schwarz, M.; Berkowitz, J. *J. Chem. Phys.* **1989**, *91* (7), 4183.

(4) Trachtman, M.; Bock, C. W.; Niki, H.; Mains, G. J. *Struct. Chem.* **1990**, *1* (2–3), 171.

(5) Curtiss, L. A.; Pople, J. A. *J. Chem. Phys.* **1989**, *91* (7), 4189.

(6) Yan-Bo, S.; Ze-Sheng, L. I.; Xu-Ri, H.; Chia-Chung, S. *Chem. J. Chin. Univ.* **2002**, *23* (8), 1542.

(7) Yan-Bo, S.; Di, W.; Ze-Sheng, L. I.; Xu-Ri, H.; Chia-Chung, S. *Chem. J. Chin. Univ.* **2002**, *23* (9), 1727.

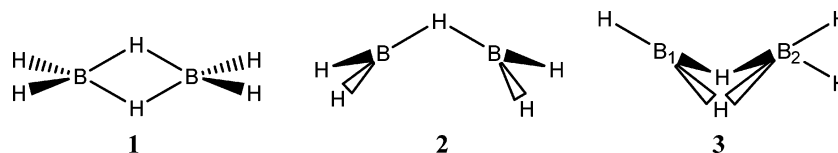


**Figure 1.** Structures of diborane (1) and of the mono- (2) and dibridged  $B_2H_5$  radicals (3).

In this Article, we present the first experimental spectroscopic characterization of the monobridged  $B_2H_5$  isomer together with its deuterated counterpart. These results provide potential insights for an identification of products and reactive intermediates in CVD processes and further experimental verification of studies concerning the minimum-energy structure of the  $B_2H_5$  potential energy surface.

## 2. Experimental Methods

Experiments were conducted using a surface scattering machine; the experimental setup has been fully explained previously.<sup>8</sup> In brief, the main chamber of the machine consists of a contamination-free ultrahigh vacuum (UHV) setup evacuated to  $10^{-10}$  Torr by a magnetically suspended turbopump, which is backed by an oil-free scroll pump. A polished silver monocrystal used for the condensation of diborane is cooled to  $11.8 \pm 0.3$  K via a rotatable, two-stage closed-cycle helium refrigerator. Diborane gas is contained initially in an adjacent gas reservoir; the condensation onto the crystal in the main chamber is controlled by a precision leak valve. During deposition, the valve is extended to 5 mm from the crystal, ensuring reproducible frost thicknesses. Frosts were prepared in separate experiments for both diborane and diborane- $d_6$  ( $B_2D_6$ ). Diborane frosts were condensed from electronic grade diborane (10%) in hydrogen, available from Aldrich Chemical Co., Inc.; diborane- $d_6$  frosts were deposited from diborane- $d_6$  (10%) in deuterium obtained from the same company. All frosts were condensed onto the silver crystal at 10 K while keeping the pressure inside the main chamber to  $10^{-5}$  Torr; since hydrogen and deuterium gases do not condense at 10 K, pure diborane ices were obtained. For a quantitative determination of diborane frost thicknesses, the 2608 and 1170  $cm^{-1}$  absorption bands were integrated and the thickness was calculated according to Bennett et al.<sup>8,9</sup> This gave sample thicknesses of about  $27 \pm 4$  nm. These frosts were irradiated for 1 h with energetic (5 keV) electrons at a nominal beam current of 1000 nA. The chemical changes inside the low-temperature diborane ices were monitored using Fourier transform infrared spectroscopy (FT-IR). The Nicolet 6700 FT-IR (8000–400  $cm^{-1}$ ) monitored the solid state at a resolution of 2  $cm^{-1}$  with time-averaged spectra recorded every 120 s.

## 3. Theoretical Methods

Harmonic vibrational frequencies of diborane, diboranyl radicals, and their isotopomers were computed at the hybrid density functional B3LYP/6-311G\*\* level<sup>10</sup> utilizing the Gaussian 98 program package.<sup>11</sup> Anharmonic (fundamental) frequencies of  $B_2H_6$  and  $B_2H_5$  were calculated at the same theoretical level using the Gaussian 03 program package.<sup>12</sup> The harmonic approximation usually employed for calculations of vibrational frequencies almost always overestimates experimental frequencies by up to 10% depending on the method of ab initio calculations (by 2–4% at

the B3LYP level).<sup>13</sup> A useful approach widely utilized to correct this deficiency is given by scaling procedures;<sup>14</sup> for instance, since calculated harmonic frequencies are generally larger than the observed fundamental frequencies, the calculated values are scaled by a factor normally in the range of 0.89–0.99.<sup>13</sup> In recent years, alternative procedures have been developed for anharmonic vibrational calculations, which directly provide fundamental frequencies by computing anharmonic corrections through second-order perturbative<sup>15</sup> or variational methodologies.<sup>16</sup> Although the second-order perturbative approach is somewhat less accurate than the variational method, it is much more computationally efficient and has been coded in the Gaussian 03 package. Since then, this method was applied for calculations of anharmonic frequencies for a variety of medium size molecules.<sup>17</sup> It has been found that the deviations of calculated anharmonic frequencies from experimental fundamental frequencies normally do not exceed 2%; however, since the computed anharmonic corrections may be either slightly underestimated or overestimated, theoretical frequencies may deviate from experiment in both directions, i.e., be either slightly higher or lower than the observed values.<sup>17</sup> This means that, if one tries to scale calculated anharmonic frequencies to match them with experiment, scaling factors varying from about 0.97 to 1.03 may be obtained.

- (11) Frisch, M. J.; Trucks, G. W.; Schlegel, H. B.; Scuseria, G. E.; Robb, M. A.; Cheeseman, J. R.; Zakrzewski, V. G.; Montgomery, J. A., Jr.; Stratmann, R. E.; Burant, J. C.; Dapprich, S.; Millam, J. M.; Daniels, A. D.; Kudin, K. N.; Strain, M. C.; Farkas, O.; Tomasi, J.; Barone, V.; Cossi, M.; Cammi, R.; Mennucci, B.; Pomelli, C.; Adamo, C.; Clifford, S.; Ochterski, J.; Petersson, G. A.; Ayala, P. Y.; Cui, Q.; Morokuma, K.; Malick, D. K.; Rabuck, A. D.; Raghavachari, K.; Foresman, J. B.; Cioslowski, J.; Ortiz, J. V.; Baboul, A. G.; Stefanov, B. B.; Liu, G.; Liashenko, A.; Piskorz, P.; Komaromi, I.; Gomperts, R.; Martin, R. L.; Fox, D. J.; Keith, T.; Al-Laham, M. A.; Peng, C. Y.; Nanayakkara, A.; Gonzalez, C.; Challacombe, M.; Gill, P. M. W.; Johnson, B.; Chen, W.; Wong, M. W.; Andres, J. L.; Head-Gordon, M.; Replogle, E. S.; Pople, J. A. *Gaussian 98*, revision A.9; Gaussian, Inc.: Pittsburgh, PA, 1998.
- (12) Frisch, M. J.; Trucks, G. W.; Schlegel, H. B.; Scuseria, G. E.; Robb, M. A.; Cheeseman, J. R.; Montgomery, J. A., Jr.; Vreven, T.; Kudin, K. N.; Burant, J. C.; Millam, J. M.; Iyengar, S. S.; Tomasi, J.; Barone, V.; Mennucci, B.; Cossi, M.; Scalmani, G.; Rega, N.; Petersson, G. A.; Nakatsuji, H.; Hada, M.; Ehara, M.; Toyota, K.; Fukuda, R.; Hasegawa, J.; Ishida, M.; Nakajima, T.; Honda, Y.; Kitao, O.; Nakai, H.; Klene, M.; Li, X.; Knox, J. E.; Hratchian, H. P.; Cross, J. B.; Adamo, C.; Jaramillo, J.; Gomperts, R.; Stratmann, R. E.; Yazyev, O.; Austin, A. J.; Cammi, R.; Pomelli, C.; Ochterski, J. W.; Ayala, P. Y.; Morokuma, K.; Voth, G. A.; Salvador, P.; Dannenberg, J. J.; Zakrzewski, V. G.; Dapprich, S.; Daniels, A. D.; Strain, M. C.; Farkas, O.; Malick, D. K.; Rabuck, A. D.; Raghavachari, K.; Foresman, J. B.; Ortiz, J. V.; Cui, Q.; Baboul, A. G.; Clifford, S.; Cioslowski, J.; Stefanov, B. B.; Liu, G.; Liashenko, A.; Piskorz, P.; Komaromi, I.; Martin, R. L.; Fox, D. J.; Keith, T.; Al-Laham, M. A.; Peng, C. Y.; Nanayakkara, A.; Challacombe, M.; Gill, P. M. W.; Johnson, B.; Chen, W.; Wong, M. W.; Gonzalez, C.; Pople, J. A. *Gaussian 03*, revision B.04; Gaussian, Inc.: Pittsburgh, PA, 2003.
- (13) Scott, A. P.; Radom, L. *J. Phys. Chem.* **1996**, *100*, 16502.
- (14) Rauhut, G.; Pulay, P. *J. Phys. Chem.* **1995**, *99*, 3039.
- (15) Barone, V. *J. Chem. Phys.* **2005**, *122*, 014108.
- (16) (a) Bowman, J. M. *Acc. Chem. Res.* **1986**, *19*, 202. (b) Gerber, R. B.; Ratner, M. A. *Adv. Chem. Phys.* **1988**, *70*, 97. (c) Carter, S.; Bowman, J. M.; Handy, N. C. *Theor. Chem. Acc.* **1998**, *100*, 191.
- (17) Alparone, A. *Chem. Phys.* **2006**, *327*, 127 and references therein.

(8) Bennett, C. J.; Jamieson, C.; Mebel, A. M.; Kaiser, R. I. *Phys. Chem. Chem. Phys.* **2004**, *6*, 735.

(9) Duncan, J. L.; McKean, D. C.; Torto, I. *J. Mol. Spectrosc.* **1981**, *85*, 16.

(10) Becke, A. D. *J. Chem. Phys.* **1993**, *98*, 5648. Lee, C.; Yang, W.; Parr, R. G. *Phys. Rev. B* **1988**, *37*, 785.

**Table 1.** Unscaled Theoretical Harmonic Frequencies (cm<sup>-1</sup>) and Infrared Intensities (km mol<sup>-1</sup>) of the Monobridged Diboranyl Radical Computed at the B3LYP/6-311G\*\* Level<sup>a</sup>

		position	intensity	position	intensity
<b><sup>11</sup>B<sub>2</sub>H<sub>5</sub></b>					
$\nu_1$	b <sub>1</sub>	2745 (2606)	149	2062 (1989)	87
$\nu_2$	a <sub>2</sub>	2727 (2605)	0	2046 (1992)	0
$\nu_3$	a <sub>1</sub>	2618 (2520)	5	1892 (1849)	4
$\nu_4$	b <sub>2</sub>	2606 (2505)	80	1875 (1828)	62
$\nu_5$	a <sub>1</sub>	1863 (1748)	10	1367 (1299)	7
$\nu_6$	b <sub>2</sub>	1716 (1622)	391	1235 (1122)	224
$\nu_7$	a <sub>1</sub>	1153 (1124)	8	881 (859)	3
$\nu_8$	b <sub>2</sub>	1117 (1078)	103	838 (818)	48
$\nu_9$	b <sub>1</sub>	993 (964)	5	719 (699)	3
$\nu_{10}$	a <sub>1</sub>	913 (891)	5	749 (731)	3
$\nu_{11}$	a <sub>2</sub>	885 (896)	0	680 (771)	0
$\nu_{12}$	b <sub>2</sub>	793 (762)	5	643 (624)	2
$\nu_{13}$	a <sub>1</sub>	662 (665)	4	543 (530)	3
$\nu_{14}$	b <sub>1</sub>	435 (457)	2	308 (318)	1
$\nu_{15}$	a <sub>2</sub>	164 (251)	0	120 (161)	0
<b><sup>11</sup>B<sup>10</sup>BH<sub>5</sub></b>					
$\nu_1$	a''	2757	131	2080	69
$\nu_2$	a''	2732	20	2052	19
$\nu_3$	a'	2621	8	1897	7
$\nu_4$	a'	2608	80	1877	62
$\nu_5$	a'	1866	10	1372	8
$\nu_6$	a'	1717	395	1237	227
$\nu_7$	a'	1157	9	891	3
$\nu_8$	a'	1121	102	842	47
$\nu_9$	a''	995	5	721	3
$\nu_{10}$	a'	921	5	756	3
$\nu_{11}$	a''	889	0	684	0
$\nu_{12}$	a'	799	5	651	2
$\nu_{13}$	a'	672	5	547	3
$\nu_{14}$	a''	434	2	308	1
$\nu_{15}$	a''	160	0	118	0
<b><sup>10</sup>B<sub>2</sub>H<sub>5</sub></b>					
$\nu_1$	b <sub>1</sub>	2762	151	2085	89
$\nu_2$	a <sub>2</sub>	2743	0	2069	6
$\nu_3$	a <sub>1</sub>	2623	5	1901	5
$\nu_4$	b <sub>2</sub>	2610	84	1881	67
$\nu_5$	a <sub>1</sub>	1870	11	1376	8
$\nu_6$	b <sub>2</sub>	1719	397	1240	229
$\nu_7$	a <sub>1</sub>	1160	8	900	3
$\nu_8$	b <sub>2</sub>	1125	102	846	47
$\nu_9$	b <sub>1</sub>	996	5	722	3
$\nu_{10}$	a <sub>1</sub>	929	4	762	3
$\nu_{11}$	a <sub>2</sub>	893	0	689	0
$\nu_{12}$	b <sub>2</sub>	805	5	658	2
$\nu_{13}$	a <sub>1</sub>	681	5	550	3
$\nu_{14}$	b <sub>1</sub>	434	2	308	1
$\nu_{15}$	a <sub>2</sub>	161	0	118	0

<sup>a</sup> Peak positions and intensities for the deuterated isomers are also included. Calculated anharmonic (fundamental) frequencies are given in parentheses.

#### 4. Experimental Results and Discussion

During the irradiation exposure of the diborane sample, new absorption features appeared at 1033 and 1398/1395 cm<sup>-1</sup>. In the corresponding diborane-*d*<sub>6</sub> ices, we found five novel absorption features at 823, 1056, 1154, 1307, and 1487 cm<sup>-1</sup>. We compare now the position of these new absorptions with the theoretically calculated absorptions (Tables 1–3). First of all, we need a calibration of the degree of anharmonicities of the computed data and the inherent scaling factors. Since the fundamentals of the diborane and diborane-*d*<sub>6</sub> molecule have been well studied in the gas phase,<sup>18</sup> we can compare the NIST data with the computed absorptions compiled in Table 3. A comparison of the computed data of the closed shell diborane molecules with the NIST based

experimental data recommends scaling factors between 0.97 and 0.99; note that the  $\nu_8$  and  $\nu_9$  fundamentals represent exceptions, and scaling factors of 0.93–0.94 are needed clearly indicating that anharmonic corrections should be significant for these vibrations. We can utilize these scaling factors to compare the theoretically predicted wavenumbers with the position of the newly observed absorption features. As indicated in Table 1, the band position corresponding to the two strongest infrared intensities for monobridged B<sub>2</sub>H<sub>5</sub> are 2745 cm<sup>-1</sup> ( $\nu_1$ ) and 1716 cm<sup>-1</sup> ( $\nu_6$ ); these peaks could not be observed since they overlapped with the  $\nu_1$  and  $\nu_8$  fundamentals of the diborane molecule. However, the third most intense peak for monobridged the B<sub>2</sub>H<sub>5</sub> isomer,  $\nu_8$ , should fall in a region in which no potentially conflicting diborane peaks are predicted to exist. As a matter of fact, a strong band was observed at 1033 cm<sup>-1</sup> (Figure 2) which can be assigned to the  $\nu_8$  mode of the monobridged diboranyl radical. We can integrate this peak at different irradiation times and plot the integrated intensity versus the irradiation time (Figure 3). Pseudo-first-order kinetics  $A_1 \xrightarrow{k} A_2$ , where  $A_1$  is the diborane molecule and  $A_2$  the monobridged B<sub>2</sub>H<sub>5</sub> isomer, were employed to fit the data. The solution to this rate law follows via  $[A_2] = a(1 - e^{-kt})$ . The corresponding fit of temporal evolution of the column density of the monobridged diboranyl radical at 1033 cm<sup>-1</sup> is shown in Figure 3; the rate constant  $k$  was calculated as  $(2.13 \pm 0.18) \times 10^{-3} \text{ s}^{-1}$ . These patterns suggest that the monobridged diboranyl radical is formed via unimolecular decomposition of an energized (internally excited) diborane molecule. For a further verification of diboranyl radical assignments, additional experiments were conducted on diborane-*d*<sub>6</sub>. Three peaks of the monobridged radical were detected via its most intense absorption at 1154 cm<sup>-1</sup> ( $\nu_6$ ), as well as at 823 cm<sup>-1</sup> ( $\nu_8$ ) and 1307 cm<sup>-1</sup> ( $\nu_5$ ) (Figure 2).

We also conducted computations of the anharmonic vibrational modes. Here, the agreement of the monobridged B<sub>2</sub>H<sub>5</sub> radical is very good showing the deviation of only 45 cm<sup>-1</sup> with scaling factors of 0.96 for  $\nu_8$  (anharmonic frequency: 1078 cm<sup>-1</sup>). The corresponding D5-isotopomer shows computed wavenumbers of 818, 1122, and 1299 cm<sup>-1</sup>; here, reasonable scaling factors of 1.01–1.03 are necessary to match the experiments with the computations. The values of scaling factors larger than 1 indicate that the present calculations overestimate anharmonic corrections, giving anharmonic frequencies slightly lower than those observed in experiment (section 3). The assignments of these absorptions can be also validated energetically. Since the monobridged isomer is expected to be more stable by about 20 kJ mol<sup>-1</sup> compared to the dibridged structure, we would expect, as verified experimentally, that during the unimolecular decomposition of diborane, the monobridged isomer should be formed preferentially.

We would like to stress that we have no definite detection of the dibridged B<sub>2</sub>H<sub>5</sub> isomer. Only very weak absorption bands were observed at 1398/1395 cm<sup>-1</sup>. In the perdeuterated

(18) NIST Atomic Spectra Database, version 3.0.; [http://physics.nist.gov/cgi-bin/AtData/main\\_asd](http://physics.nist.gov/cgi-bin/AtData/main_asd) (accessed February 2005).

**Table 2.** Unscaled Theoretical Harmonic Frequencies ( $\text{cm}^{-1}$ ) and Infrared Intensities ( $\text{km mol}^{-1}$ ) of the Dibridged Diboranyl Radical Computed at the B3LYP/6-311G\*\* Level<sup>a</sup>

		position	intensity	position	intensity	position	intensity	position	intensity
		<sup>11</sup> B <sub>2</sub> H <sub>5</sub>		<sup>11</sup> B <sub>2</sub> D <sub>5</sub>		<sup>10</sup> B <sub>2</sub> H <sub>5</sub>		<sup>10</sup> B <sub>2</sub> D <sub>5</sub>	
$\nu_1$	a'	2702 (2610)	70	2002 (1941)	60	2714	73	2024	50
$\nu_2$	a'	2673 (2563)	63	1999 (1946)	18	2689	63	2017	31
$\nu_3$	a'	2579 (2478)	68	1866 (1819)	49	2585	71	1875	53
$\nu_4$	a'	2212 (2142)	20	1572 (1463)	11	2213	20	1574	11
$\nu_5$	a''	2103 (2009)	0	1553 (1498)	0	2113	0	1566	0
$\nu_6$	a''	1643 (1359)	1	1191 (1049)	1	1647	1	1197	1
$\nu_7$	a'	1485 (1214)	210	1083 (951)	118	1490	212	1089	120
$\nu_8$	a'	1173 (1142)	36	894 (873)	13	1179	36	915	11
$\nu_9$	a''	969 (942)	11	743 (729)	7	977	11	754	7
$\nu_{10}$	a'	914 (893)	1	781 (757)	1	929	0	796	1
$\nu_{11}$	a'	865 (845)	3	710 (695)	1	892	3	722	1
$\nu_{12}$	a''	844 (791)	1	637 (613)	0	846	0	643	0
$\nu_{13}$	a''	831 (763)	0	596 (556)	0	838	0	596	0
$\nu_{14}$	a'	658 (541)	0	505 (433)	1	666	0	511	1
$\nu_{15}$	a'	410 (402)	20	296 (295)	11	412	21	296	11
		<sup>11</sup> B <sup>10</sup> BH <sub>5</sub> <sup>b</sup>		<sup>11</sup> B <sup>10</sup> BD <sub>5</sub> <sup>b</sup>		<sup>11</sup> B <sup>10</sup> BH <sub>5</sub> <sup>c</sup>		<sup>11</sup> B <sup>10</sup> BD <sub>5</sub> <sup>c</sup>	
$\nu_1$	a'	2714	69	2017	43	2702	80	2024	45
$\nu_2$	a'	2673	66	2001	38	2688	53	2000	34
$\nu_3$	a'	2579	69	1866	49	2585	72	1875	53
$\nu_4$	a'	2213	20	1574	11	2212	20	1572	11
$\nu_5$	a''	2111	0	1563	0	2105	0	1555	0
$\nu_6$	a''	1643	1	1191	1	1647	1	1197	1
$\nu_7$	a'	1488	210	1085	117	1487	213	1086	121
$\nu_8$	a'	1173	37	898	14	1179	36	910	11
$\nu_9$	a''	969	11	743	6	977	11	753	7
$\nu_{10}$	a'	919	0	793	1	923	1	784	1
$\nu_{11}$	a'	878	4	714	1	880	3	718	1
$\nu_{12}$	a''	846	0	643	0	845	0	637	0
$\nu_{13}$	a''	836	0	596	0	834	0	596	0
$\nu_{14}$	a'	666	0	511	1	659	0	506	1
$\nu_{15}$	a'	411	21	297	11	411	20	296	11

<sup>a</sup> Peak positions and intensities for the deuterated isomers are also included. Calculated anharmonic (fundamental) frequencies are given in parentheses. <sup>b</sup> <sup>10</sup>B at B<sub>1</sub> (see Figure 1). <sup>c</sup> <sup>10</sup>B at B<sub>2</sub> (see Figure 1).

**Table 3.** Unscaled Harmonic Frequencies ( $\text{cm}^{-1}$ ) and Infrared Intensities ( $\text{km mol}^{-1}$ ) of Diborane Computed at the B3LYP/6-311G\*\* Level<sup>a</sup>

		<sup>11</sup> B <sub>2</sub> H <sub>6</sub>		<sup>10</sup> B <sub>2</sub> H <sub>6</sub>		<sup>11</sup> B <sub>2</sub> D <sub>6</sub>		<sup>10</sup> B <sub>2</sub> D <sub>6</sub>	
		band position	intensity	band position	intensity	band position	intensity	band position	intensity
$\nu_1$	b <sub>2u</sub>	2705 (2604)	179	2721	181	2025	100	2047	103
$\nu_2$	b <sub>1g</sub>	2691 (2586)	0	2707	0	2018	0	2040	0
$\nu_3$	a <sub>g</sub>	2614 (2522)	0	2620	0	1898	0	1909	0
$\nu_4$	b <sub>3u</sub>	2601 (2510)	146	2606	153	1878	112	1886	121
$\nu_5$	a <sub>g</sub>	2164 (2087)	0	2164	0	1536	0	1537	0
$\nu_6$	b <sub>1u</sub>	1978 (1818)	9	1989	9	1477	7	1493	7
$\nu_7$	b <sub>2g</sub>	1843 (1710)	0	1846	0	1322	0	1327	0
$\nu_8$	b <sub>3u</sub>	1700 (1528)	471	1705	478	1239	266	1247	271
$\nu_9$	a <sub>g</sub>	1199 (1164)	0	1205	0	915	0	935	0
$\nu_{10}$	b <sub>3u</sub>	1190 (1157)	77	1196	74	882	26	888	24
$\nu_{11}$	b <sub>3g</sub>	1022 (979)	0	1022	0	723	0	723	0
$\nu_{12}$	b <sub>1u</sub>	990 (966)	17	995	17	731	9	736	9
$\nu_{13}$	b <sub>2u</sub>	951 (917)	0	955	0	700	0	705	0
$\nu_{14}$	b <sub>1g</sub>	937 (910)	0	951	0	747	0	760	0
$\nu_{15}$	b <sub>2g</sub>	890 (851)	0	905	0	729	0	747	0
$\nu_{16}$	a <sub>u</sub>	848 (817)	0	848	0	600	0	600	0
$\nu_{17}$	a <sub>g</sub>	796 (760)	0	828	0	716	0	730	0
$\nu_{18}$	b <sub>2u</sub>	358 (329)	16	358	17	253	8	253	8

<sup>a</sup> Calculated anharmonic (fundamental) frequencies are given in parentheses.

samples, minor absorptions appear which could be tentatively assigned at  $1056 \text{ cm}^{-1}$  ( $\nu_7$ ) and at  $1487 \text{ cm}^{-1}$  ( $\nu_4$ ). However, in strong contrast to the monobridged isomer, a comparison of the experimental data with the scaled, calculated frequencies does not permit a definite conclusion. Therefore, we must conclude that in our experiments we only observed, by a comparison of the scaled, computed frequencies with the experimental data, the monobridged isomer.

Can other species account for the experimentally observed absorptions? It should be noted that the first step in an

energetic electron-induced unimolecular decomposition of related main group IV hydrides methane ( $\text{CH}_4$ ),<sup>19</sup> silane ( $\text{SiH}_4$ ),<sup>20</sup> and germane ( $\text{GeH}_4$ )<sup>21</sup> was found to be an initial formation of the corresponding  $\text{EH}_3$  ( $\text{E} = \text{C}, \text{Si}, \text{Ge}$ ) radical plus atomic hydrogen; the temporal profiles of these radicals

(19) Bennett, C. J.; Jamieson, C. S.; Osamura, Y.; Kaiser, R. I. *Astrophys. J.* **2006**, 653, 792.

(20) Sillars, D.; Bennett, C. J.; Osamura, Y.; Kaiser, R. I. *Chem. Phys.* **2004**, 305, 143.

(21) Carrier, W.; Zheng, W.; Osamura, Y.; Kaiser, R. I. *Chem. Phys.* **2006**, 325, 499.

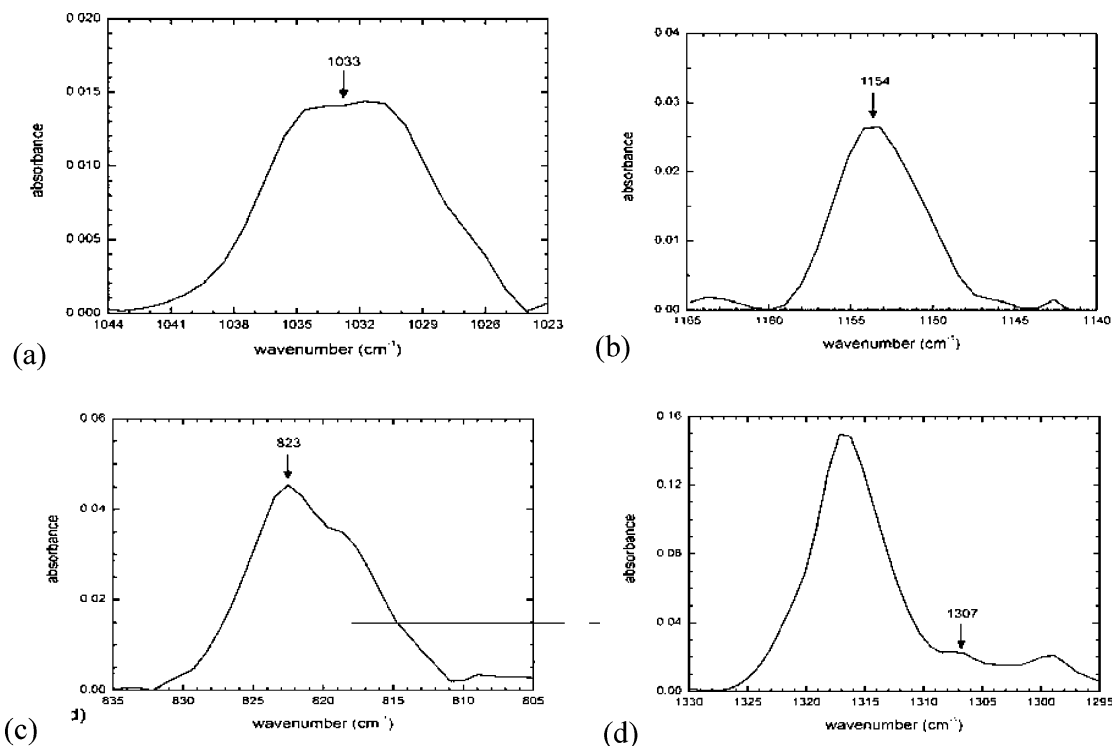


**Figure 2.** Experimentally observed absorption features corresponding to (a) monobridged  $B_2H_5$  and (b–d) monobridged  $B_2D_5$  radicals formed during irradiation of diborane and diborane- $d_6$  ices at 10 K. The unassigned peaks belong to the  $B_2H_6$  and  $B_2D_6$  reactants.

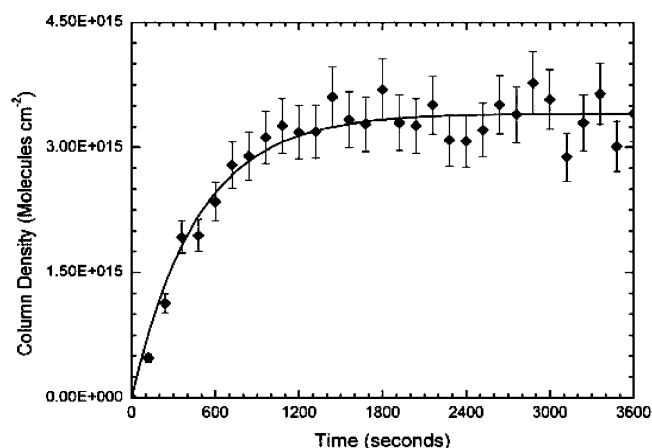


**Figure 3.** Plots of the evolution of the column density (molecules  $cm^{-2}$ ) with respect to time for the experimentally observed absorption of the  $1033\text{ cm}^{-1}$  band for the monobridged  $B_2H_5$  isomer.

could all be fit with pseudo-first-order kinetics. This is in analogy to the monobridged  $B_2H_5$  radical observed in the present system. Therefore, we can conclude that at least under the experimental conditions of the present studies, the monobridged  $B_2H_5$  radical is formed but no other higher order irradiation products.

## 5. Conclusions

The monobridged  $B_2H_5$  radical has been identified experimentally for the first time in low-temperature diborane ices at 10 K. We characterized the absorptions of the monobridged  $B_2H_5$  structure at  $1033\text{ cm}^{-1}$  ( $\nu_8$ ). This absorption was verified by characterization of the corresponding  $B_2D_5$  isomer in diborane- $d_6$  ices. For the monobridged  $B_2D_5$ , three fundamentals were detected at  $1154$  ( $\nu_6$ ),  $823$  ( $\nu_8$ ), and

$1307$  ( $\nu_5$ )  $cm^{-1}$ . The temporal evolution of the absorption shows that this radical is formed via unimolecular decomposition of the diborane molecule. It is interesting to note that the related  $Al_2H_5$  system energetically favors the dibridged isomer compared to the monobridged structure.<sup>22</sup> This reflects a common trend of hydrogen deficient, main group hydrides to favor (di)bridged structures when going to the higher homologues within a group. This has been found, for example, also in acetylene ( $C_2H_2$ ) versus disilacetylene ( $Si_2H_2$ )<sup>23</sup> and digermacetylene ( $Ge_2H_2$ )<sup>24</sup> where acetylene is linear, but both latter structures prefer a dibridged arrangement of the hydrogen atoms.

**Acknowledgment.** We thank Chris Bennett (UH) for assistance with the experimental procedures. The experimental work was funded by the Air Force Office of Scientific Research (Grant W911NF-05-1-0448; R.I.K.) and by the National Science Foundation Research Experience for Undergraduates (J.G.L.). A.M.M. thanks Institute of Atomic Molecular Science, Academia Sinica, in Taipei, for the use of their computer cluster and the Gaussian 03 program package for calculations of anharmonic frequencies. R.I.K. thanks Prof. Holger Bettinger (University of Bochum, Germany) for discussions.

IC0622712

(22) Andrews, L.; Wang, X. *J. Phys. Chem. A* **2004**, *108*, 4202.

(23) Osamura, Y.; Kaiser, R. I. *Astrochemistry: From Laboratory Studies to Astronomical Observations, Honolulu, Hawaii, 18–20 December 2005*; Kaiser, R. I., Ed.; American Institute of Physics: Melville, NY, 2006; Vol. 855, p 289.

(24) Carrier, W.; Zheng, W.; Osamura, Y.; Kaiser, R. I. *Chem. Phys.* **2006**, *330*, 275.